Heliyon 10 (2024) e24474

Contents lists available at ScienceDirect

Heliyon

journal homepage: www.cell.com/heliyon

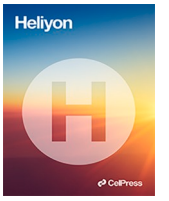

Research article

Long-term spatiotemporal dynamics of groundwater storage in the data-scarce region: Tana sub-basin, Ethiopia

Kibru Gedam Berhanu [a,*], Tarun Kumar Lohani [b], Samuel Dagalo Hatiye [a]

[a] Arba Minch Water Technology Institute, Faculty of Water Resources and Irrigation Engineering, Arba Minch University, Arba Minch, Ethiopia
[b] Arba Minch Water Technology Institute, Faculty of Hydraulic and Water Resources Engineering, Arba Minch University, Arba Minch, Ethiopia

ARTICLE INFO

Keywords:
Groundwater storage change
Spatiotemporal
GRACE
GLDAS
Trend analysis
Tana sub-basin

ABSTRACT

Imprudent extraction of groundwater tends to undue stress and portends its sustainability. Spatiotemporal analysis of groundwater storage anomaly (GWSA) is imperative for the judicious use, management, and sustainable development of a region. This study aimed to examine the changes in groundwater storage over the past 20 years in the Tana sub-basin using Gravity Recovery and Climate Experiment (GRACE) assimilated into Global Land Data Assimilation Systems (GLDAS). Validation analysis was carried out to evaluate the accuracy of GWSA against anomalies of Lake Tana water level, precipitation, and in-situ groundwater level. Modified Mann-Kendal test and Sen's slope estimator were applied for trend analysis of the GWSA. The results exhibited that GWSA strongly correlated (Pearson's correlation coefficient, R ranges from 0.75 to 0.96) with the three validation above variables, which elucidated in general, credible GWSA estimation. The net annual GWSA curve showed a non-significant ($p > 0.05$) decreasing trend from 2003 to 2012. However, years including 2005, 2006, and 2009 were drought periods, which caused 0.49 billion cubic meters (BCM) groundwater loss. In the entire study period (2003–2022), on the other hand, the net annual GWSA revealed a significant increasing trend ($p < 0.05$) with a rate of 0.333 cm/year. Generally, the Tana sub-basin was nurtured with a net 4.87 BCM groundwater gain in the study period. The most sensitive parts of the study area to large fluctuations of groundwater storage were mainly the nearby southern and eastern directions of Lake Tana.

1. Introduction

Groundwater (GW) plays a pivotal role across the globe in nourishing domestic, agricultural, and industrial demands [1,2]. In recent years, however, the trend of using GW and stress on it has been increasing due to increased demand for massive infrastructural development and huge population growth of the world [3–6]. Quantity and quality deterioration of surface water due to anthropogenic activities, climate change, and the development of modern technology to extract GW are also prominent causes of increased use of GW worldwide [7–9]. The increase in population, urbanization, and industrialization has also led to the release of higher levels of pollutants into the environment. As a result, both the quantity and quality of groundwater resources have been negatively impacted [10]. The continuous decline of groundwater levels is caused by increasing stresses on groundwater and overexploitation, which exceeds its ability to be replenished by recharge. This phenomenon of long-term groundwater depletion is becoming more common in various countries around the world, including China, India, Saudi Arabia, the United States, Iran, the Arabian Peninsula, and some African

* Corresponding author.
E-mail address: kibru6477@gmail.com (K.G. Berhanu).

https://doi.org/10.1016/j.heliyon.2024.e24474
Received 13 July 2023; Received in revised form 6 January 2024; Accepted 9 January 2024

countries [11–13]. Therefore, a lesson should be taken from the aforementioned regions before groundwater depletion becomes a worse condition in other countries for sustainable utilization and development of the nation.

Ethiopia is endowed with water resources and is considered a water tower of Africa that has approximately 252 billion cubic meters (BCM) of water resources available with rivers, lakes and groundwater [14,15]. Nonetheless, the groundwater quantity studies in Ethiopia showed that there is no agreed quantity available yet. For example, the Ethiopian Ministry of Water Resources (MoWR) [16] carried out the countrywide preliminary water resources master plan study and estimated it as 2.6 BCM. Alemayehu [17], on the other hand, estimated it to be around 185 BCM. A more recent study also speculated the groundwater reserve of Ethiopia as 12 BCM to 30 BCM or even more [15]. These are pieces of evidence that there is no agreed understanding of the quantity of groundwater available in Ethiopia.

These huge discrepancies among estimated figures reveal that more detailed investigations are still needed for sustainable utilization and management of this precious resource. Lack of concrete information on the availability of GW reserve hampers, on one hand, its full-scale utilization for different proposes, and on the other hand, endangers its sustainability when it is unknowingly overexploited. For example, the dearth of GW availability information limited its use for irrigation to less than 5 % of the country's irrigable land [15,18,19] whereas 85 % for domestic water supply [20].

Tana sub-basin (study area), which is found in the Upper Blue Nile, has a huge groundwater reserve [21–23]. Nevertheless, increasing use of groundwater has been recorded in different sectors leading to groundwater level decline [24–27]. The study area's groundwater is confirmed by many researchers that it has high connectivity with rivers and it feeds rivers and Lake Tana via base flow [25,28–30]. Therefore, the reduction of the groundwater table not only harms the groundwater resources but also the surface water resources to dry up and decrease flow. It is known that Lake Tana is the womb of the Abay River (Blue Nile River) on which the Grand Ethiopian Renaissance Dam (GERD) is under construction. In this regard, the long-term investigation of the groundwater storage change and its variability is imperative for thoughtful integrated groundwater and surface water development and management sustainably [31].

To carry out long-term groundwater storage dynamics, sufficient and plausible in-situ measured time series data is required. Unfortunately, in developing countries like Ethiopia, scarcity of in-situ GW monitoring is commonplace due to financial constraints. Tana sub-basin is one of the regions where a groundwater monitoring system has not been established yet. Therefore, finding another option to get reliable information is vital for GW storage change studies.

Gravity Recovery and Climate Experiment (GRACE)/and its successor GRACE-Follow On (GRACE-FO) is one of the emerging remote sensing technologies widely used to successfully estimate GW storage anomaly (GWSA) [13,32]. It has brought a new dimension to evaluate GWSA changes in the large and small spatial scales of any hotspot region. For instance, GRACE-based GWSA

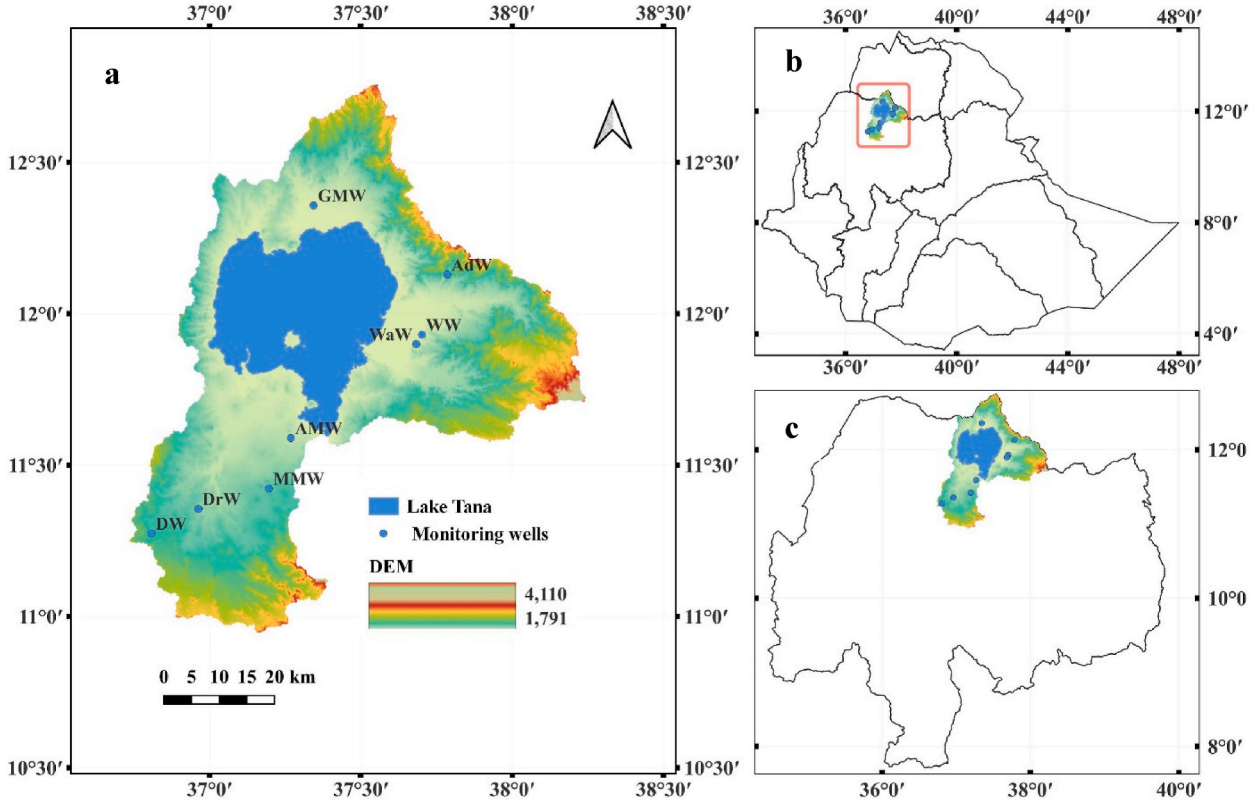

Fig. 1. Study area (a), Ethiopia and its major basins (b), and Upper Blue Nile Basin (c).

studies were carried out in large regions, such as the Middle East, India, China, Australia, and the United [11,33]. Estimation of GW depletion in Brazil [34] and GW (including soil moisture) changes in Ethiopia were a few evidences that GRACE data can also be applied to small-scale regions. In general, monitoring large-scale and small-scale GWSA studies employing GRACE/GRACE-FO changes has been increasing from time to time, thereby in-situ observation networks have been found to decline in coverage in recent years around the world [35].

However, GRACE provides only the terrestrial water storage anomaly (TWSA) of the earth, which integrates GWSA, surface water storage anomaly (SWSA), soil moisture storage anomaly (SMSA), and snow water equivalent storage change (SWESA). Global Land Data Assimilation Systems (GLDAS) land surface models have been used to disintegrate the GRACE-derived TWSA into its components and obtain GWSA. In the present study, the new version of GLDAS (GLDAS-2.2), which assimilates GRACE/GRACE-FO into the GLDAS land surface model, was employed. The specific objectives of the present study are to (1) produce the spatial and temporal GWSA variations, (2) assess the temporal GWSA trends by applying the modified Mann-Kendall's test and Sen's Slope estimator, and (3) compute the loss and or gain of groundwater in the past 20 years (2003–2022) in the data-scarce region, Lake Tana sub-basin, Ethiopia.

2. Materials and methods

2.1. Study area description

The Tana sub-basin (Fig. 1 a) is located in the northwestern part of Ethiopia (Fig. 1b) and is part of the Upper Blue Nile Basin (Fig. 1 c). It encompasses a total surface area of 15,092 km^2, with Lake Tana occupying 3047 km^2, making it the largest lake in Ethiopia.

The climate of the study area is controlled by a tropical highland monsoon with a wet season (June–September) and dry (October–March) seasons [36,37]. The maximum mean monthly rainfall ranges from 250 to 330 mm/month during the wet season which mainly runs from July to August and the average annual rainfall reaches 1400 mm [23,38,39]. The mean annual temperature of the study area is 20 °C and it shows small seasonal variability [40]. The four major rivers feeding Lake Tana are Gilgel Abbay, Gumara, Ribb and Megech. The dominant land use/cover in the study region includes grassland, marshland, cultivated land and forest [23].

The lithological formations of the study region comprise Tarmaber basalts, volcanic center basalts, alluvium and lacustrine deposits, marsh soil, colluvium, Lateriteon Amba Alaji and Rhyolite Amba Aiba basalts [23,41,42]. There are also several soil types in the study area such as Haplic and Chromic Luvisols, Eutric soils (Leptosols, Vertisols, and Fluvisols), Lithic Leptosols, and Haplic Alisols [23,43].

2.2. Dataset and analysis

2.2.1. GRACE

The GRACE (Gravity Recovery and Climate Experiment) [44] and GRACE-Follow On (GRACE-FO) [45] provide accurate monthly earth gravity field measurements of water resources. The GRACE and GRACE-FO satellite datasets can be accessed from the Center for Space Research (CSR), Goddard Space Flight Center (GSFC), GeoForschungs Zentrum Potsdam (GFZ), and Jet Propulsion Laboratory (JPL) in different algorithms [46,47]. This GRACE satellite dataset has two solutions, mass concentration (Mascon) and spherical harmonics (SH). The GRACE Mascon solution has less leakage than the SH solution [48,49]. Moreover, the Mascon solution does not need post-processing, filtering and has less dependency on scale factors [49,50]. Moreover, it is confirmed in the previous study that the Mascon obtained from CSR has less uncertainty than the GRACE spherical harmonics in the Nile River basin that includes the present study area [51]. Therefore, the GRACE CSR-Mascon data assimilated with the latest GLDAS land surface model [50] was employed here.

2.2.2. GLDAS

Global Land Data Assimilation System (GLDAS) data is the first global high-resolution (1°–0.25°) land surface modelling method coupling ground-based and satellite-based observations. GLDAS produces TWS (encompasses SMS, SWES, canopy water storage (CWS) and surface runoff, Qs) and other hydrological fluxes [52–54]. It currently involves five Land Surface Models (LSMs) including the Variable Infiltration Capacity (VIC) model [55], the Mosaic model (Mosaic) [56], the Community Land Model (CLM) [57], the NOAH model [58,59], and Catchment Land Surface Model (CLSM) [50].

Among the GLDAS data, GLDAS version 2.2 (GLDAS-2.2) is a unique and advanced CLSM. It provides direct daily and finer (0.25°) spatial resolution GWS data including TWS and SMS from February 2003 to the present. This latest version of the GLDAS data is produced by combining observational data, modelled data, and Data Assimilation (DA) from GRACE/GRACE = FO [50,60]. The GRACE data selected for GLDAS-2.2 DA is a CSR Mascon solution. The selection was because the CSR mascon solution has the best spatiotemporal resolution of the other GRACE products and it needs no post-processing besides its fewer leakage errors [50]. GLDAS-2.2 is critical for providing finer spatiotemporal resolution and continues direct TWS and GWS acquisition other than other GRACE and GLDAS datasets. GLDAS-2.2 eludes a data gap-filling computation for missing data between the transition period of GRACE and GRACE-FO, thereby reducing errors. It also avoids the need to calculate GLDAS-derived TWS indirectly from the individual products. Besides, using GLDAS-2.2 CLSM-derived GWS is used to circumvent mainly the SWS data gap and difficulties to obtain it from different methods for disaggregating the GRACE/GRACE-FO derived TWS components [61]. More details about GLDAS data can be found in the GLDAS 2 document [62].

GLDAS-2.2 CLSM data was accessed from (https://disc.gsfc.nasa.gov/datasets? keywords= GLDAS_CLSM025 _DA 1_D _2.2 &page = 1) website. Then, GWSA including TWSA (for comparison) covering the past two decades (2003–2022) was computed by taking a

time-mean from 2004 to 2009. Open source tools mainly Quantum Geographic Information System (QGIS) and Climate Data Operators (CDO), python, and R programming language were employed to manipulate and analyze the NetCDF datasets and statistical measures.

2.2.3. Satellite altimetry and precipitation data

Many researchers have used the satellite altimetry derived from missions including GFO, Topex-Poseidon, ERS-2, Jason version 1 and 2, and Envisat to successfully derive the water level in lakes including rivers, reservoirs, and wetlands [63–66]. In general, these satellites render water level fluctuations for around 150 reservoirs and lakes around the globe, and the datasets are available freely from http://www.logos.obs-mip.fr/soa/hydro logie/hydroweb. In the present study, the satellite altimetry data (http://www.legos.obs-mip.fr/soa/hydrologie/hydroweb/Stations Virtuelles/SV_Lakes/Tana. html) was used to augment the in-situ Tana Lake level data gaps. Daily water heights were converted to monthly changes or anomalies using baseline time from 2004 to 2009 for comparison and verification purposes for the simulated GWSA.

For a better comparison with the gridded GLDAS-2.2 derived GWSA, monthly rainfall was obtained from Climate Hazards Group Infrared Precipitation with Stations (CHIRPS) version 2.0. CHIRPS was 0.05° by 0.05-degree spatial resolution rainfall data from 1981 to present and accessed from the website (https://data.chc.ucsb.edu/products/CHIRPS-2.0/global monthly/netcdf/). CHIRPS was earlier verified by the in-situ rain gauges for Ethiopia and particularly for the present study area [67,68]. It was also verified and found a very high correlation (R = 0.99) with the rain gauges of the study area before use in the present study.

2.2.4. Ground-based measurement data

Time series groundwater level monitoring data, which coincides with GWSA, is required for validation. However, as aforementioned in the introduction section, there is no in-situ groundwater level data in Ethiopia in general and in the current study area in particular. In the current study, therefore, eight wells were monitored using a dip meter for validation purposes. The monitored wells comprised of Dangila well (DW), Durbetie well (DrW), Merawi monitoring well (MMW), Areki Minch monitoring well (AMW), Guramba monitoring well (GMW), Woreta well (WW), Woreta agricultural well (WaW), and Addis Zemen well (AdW) (Fig. 1). The first four wells were monitored weekly from July 2021 to November 2022 whereas the other remaining wells were monitored weekly from November 2021 to November 2022. The recorded water level fluctuation change (Δh) was used to compute the GWSA derived from these observation wells ($GWSA_{obs}$) by multiplying with corresponding specific yield (S_y) values (equation (1)) [69,70].

$$GWSA_{obs} = \Delta h \times S_y \tag{1}$$

The value of S_y was estimated based on the aquifer material properties [70–72]. It ranges from 0.02 to 0.3 for unconfined and from 0.0001 to 0.001 for confined aquifers [29].

Other publicly available in-situ data including daily precipitation and Tana Lake level were collected from the Ethiopian Water and Energy Ministry and National Meteorological Institute, respectively, to verify and augment the satellite data.

2.3. Trend analysis

The use of trend analysis techniques is widespread in meteorological and hydrological trend studies. These techniques include linear regression, the Mann-Kendall test [73,74], a modified version of Mann-Kendall [75], Sen's slope estimator [76], Spearman's Rho test, and innovative trend analysis are widely used in meteorological and hydrological trend studies [77–82]. The parametric linear regression tool is prone to both outliers and autocorrelation [77]. On the other hand, the non-parametric Mann-Kendall and Spearman's Rho tests are vulnerable to autocorrelation effects in time series data [77,78,81,83]. The innovative trend analysis method is imperative to aid visual understanding of trends [78], but it is not capable of providing the magnitude of significant trends [77].

The modified Mann-Kendal (MMK) is the robust method, bypasses the effect of autocorrelation, and thus provides the most credible trend analysis result [77,81,83]. The Sen's slope estimator (SS) technique is used broadly with MMK to quantify the magnitude of the significant trends [83–85]. Therefore, MMK and SS trend analysis methods were selected and employed here among the aforementioned techniques. In these methods, if the p-value is greater than 0.05, it shows no trend, and if it is less than 0.05, it shows there is a significant upward or downward trend [86,87]. The Sen's slope sign implies increasing (positive slope) and decreasing (negative slope) when the absolute value of MMK's corrected statistic (Z_c) is greater than 1.96 at a 95 % confidence interval [83,88]. The formulas (from Equations (2)–(9)) to be applied here in the trend analysis were also described in the earlier works [81,83–85].

The modified Mann Kendall's statistical S is given by equation (2):

$$S = \sum_{k-1}^{n-1} \sum_{k+1}^{n} \mathrm{Sign}\left(Y_j - Y_k\right) \tag{2}$$

where Y_j and Y_k are the time series variables at j and k sequential time, respectively and the Sign () function is defined in equation (3):

$$Sign\left(Y_j - Y_k\right) = \begin{cases} 1 \; if \; \left(Y_j - Y_k\right) > 0 \\ 0 \; if \; \left(Y_j - Y_k\right) = 0 \\ -1 \; if \left(Y_j - Y_k\right) < 0 \end{cases} \tag{3}$$

The corrected standardized MMK's test statistic (Z_c) is computed in equation (4):

$$Z_c = \begin{cases} \dfrac{S-1}{\sqrt{Vr_{mmk}(S)}}, if\ S > 0 \\ 0, if\ S = 0 \\ \dfrac{S+1}{\sqrt{Vr_{mmk}(S)}}, if\ S < 0 \end{cases} \tag{4}$$

where Vr_{mmk} (S) is MMK's statistical variance. It is the multiplication of conventional MK's variance (Vr_{mk}) by a correction factor (Cf) as follows:

$$Vr_{mmk} = Vr_{mk} \times Cf = \frac{N(N-1)(2N+5) - \sum_{i=1}^{m} d_i\ (d_i - 1)(2d_i + 5)}{18} \times Cf \tag{5}$$

where, N = total number of data points in the temporal data series, m = the number of grouped data points having the same values in the time series, and d_i = the number of data points in the ith group.

To address the issue of autocorrelation of all lags, Ac(i) in time series trend analysis, the correction factor (Cf) was introduced by Hamed and Rao [75]. It can be estimated as:

$$Cf = 1 + \frac{2}{N(N-1)(N-2)} \times \sum_{i=1}^{N-1} (N-i)(N-i-1)(N-i-2)Ac(i) \tag{6}$$

where,

$$Ac(i) = \frac{\frac{1}{N-1}\sum_{j=i+1}^{N}\left(Y_j - \overline{Y}\right)\left(Y_{j-i} - \overline{Y}\right)}{\sqrt{\frac{1}{N}\sum_{j=1}^{N}\left(Y_j - \overline{Y}\right)}\sqrt{\frac{1}{N}\sum_{j=i+1}^{N}\left(Y_{j-i} - \overline{Y}\right)}} \tag{7}$$

Sen's slope (a) is used to determine the magnitude of the linear trend line in equation (8) in the temporal dataset.

$$\mathrm{f(t)} = \mathrm{at} + \mathrm{b} \tag{8}$$

where f(t) is a function of temporal data, a is Sen's slope, and b is the intercept or constant number. The Sen's slope (a) is defined as equation (9):

$$\mathrm{a} = \mathrm{Median}\left(\frac{\mathrm{X_j} - \mathrm{X_k}}{\mathrm{j} - \mathrm{k}}\right) \text{ for all } \mathrm{j} > \mathrm{k} \tag{9}$$

The *modifiedmk* R package was applied to ease the computations in trend analysis.

2.4. Statistical measures for validation

Indices including correlation coefficient (R), coefficient of determination (R^2), and Nash-Sutclife efficiency (NSE) were applied to show the correlation between simulated GWSA with $GWSA_{obs}$.

2.4.1. Pearson's correlation coefficient (R) and coefficient of determination (R^2)

Pearson's correlation coefficient, R shows the correlation between observed data (X) and simulated data (Y). R ranges from −1 to 1 and if it is equal to −1 and 1, the observed or measured and simulated data are perfectly correlated [89]. In this study, the following R values and the corresponding interpretations were adopted and modified from [90] as $0.9 < R < 1$ (very high), $0.7 < R \leq 0.9$ (high), $0.5 < R = 0.7$ (moderate), $0.3 < R \leq 0.5$ (low), and $R \leq 0.3$ (very low). The coefficient of determination is just the square of R and generally, a 0.5 R^2 value is acceptable.

$$\mathrm{R} = \frac{\sum_{\mathrm{i=1}}^{\mathrm{N}}(\mathrm{X_i} - \overline{\mathrm{X}})(\mathrm{Y_i} - \overline{\mathrm{Y}})}{\sqrt{\sum_{\mathrm{i=1}}^{\mathrm{N}}(\mathrm{X_i} - \overline{\mathrm{X}})^2}\sum_{\mathrm{i=1}}^{\mathrm{N}}(\mathrm{Y_i} - \overline{\mathrm{Y}})^2} \tag{10}$$

Where;

X_i and Y_i are observed and simulated datasets with the mean value of $\overline{X}$ *and* $\overline{Y}$, respectively, and N is the total number of datasets.

2.4.2. Nash-sutcliffe efficiency coefficient (NSE)

The values of NSE (equation (8)) range from -∞ to 1 and if NSE is closer to 1, it reveals a better modelling accuracy and higher reliability model. Generally, if the NSE is between 0 and 1, it shows acceptable model performance whereas the 0 and negative values

are unacceptable simulated values or model performance [89].

$$\mathbf{NSE} = \mathbf{1} - \frac{\sum_{i=1}^{N} (\mathbf{X_i} - \mathbf{Y_i})^2}{\sum_{i=1}^{N} (\mathbf{X_i} - \overline{\mathbf{X}})^2} \tag{11}$$

3. Results

3.1. Temporal GWSA fluctuations

The simulated monthly GWSA time series (from 2003 to 2022) of the Tana sub-basin is depicted in Fig. 2 a. The MMK test and Sen's slope estimator trend analysis result revealed an increasingly significant trend ($p < 0.05$). The trend has a rate of 0.005 cm/month. The net annual GWSA (Fig. 2 a) also showed a significant increasing trend with a 0.333 cm/year rate. GWSA is one of the major components of the TWSA in the study region, as it could be understood from Fig. 2 b. The net annual GWSA is greatly correlated ($R = 0.998$) with the corresponding TWSA. The trend of the long-term net annual TWSA was significantly increasing as the net annual GWSA. The earlier study, which was conducted in the Blue Nile Basin (includes the current study area), from 2002 to 2020 also showed a significant increasing trend of the TWSA [60].

When the first decade (2003–2012) was considered, the net annual GWSA (Fig. 2 b) revealed a declining trend though it was not statistically significant ($p > 0.05$). The significant ($p < 0.05$) increasing trend was observed in the second decade from 2012 to 2022. The greatest fluctuation of the net annual GWSA was observed from 2004 to 2005 (−3.05 cm/year), 2006 to 2007 (2.93 cm/year), and from 2018 to 2019 raised at a rate of 3.54 cm/year. The net annual GWSA time series (Fig. 2 b) also revealed that three years (2005, 2006, and 2009) were dry triggering a 0.49 BCM groundwater deficit. This was mainly related to the decrement in precipitation and Tana Lake levels (Fig. 5a and 5 b) caused by droughts that occurred in the preceding years as pointed out by previous studies [21,91, 92]. Nevertheless, in the entire study period (2003–2022), the study area experienced a net gain of 40.43 cm of groundwater. Considering the Tana sub-basin area as 12,045 km^2 (without Lake Tana area), the total gain of groundwater was 4.87 BCM for the past

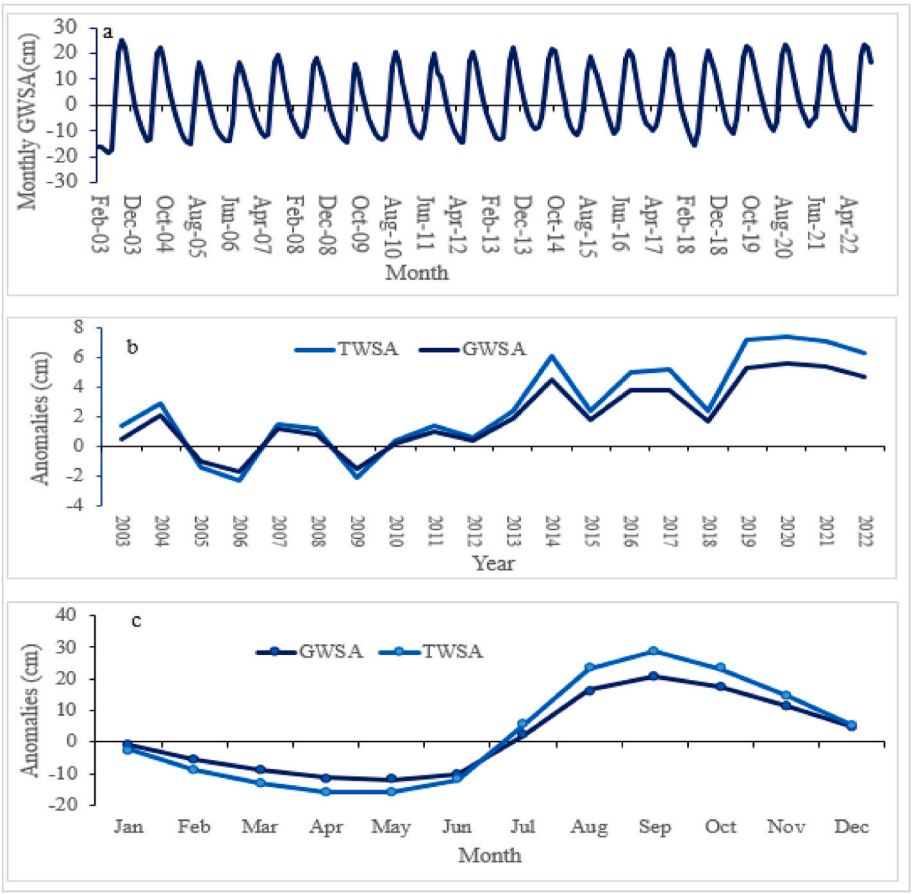

Fig. 2. Monthly GWSA (a), net annual GWSA and TWSA (b), and the study period monthly mean of GWSA and TWSA for comparison (c).

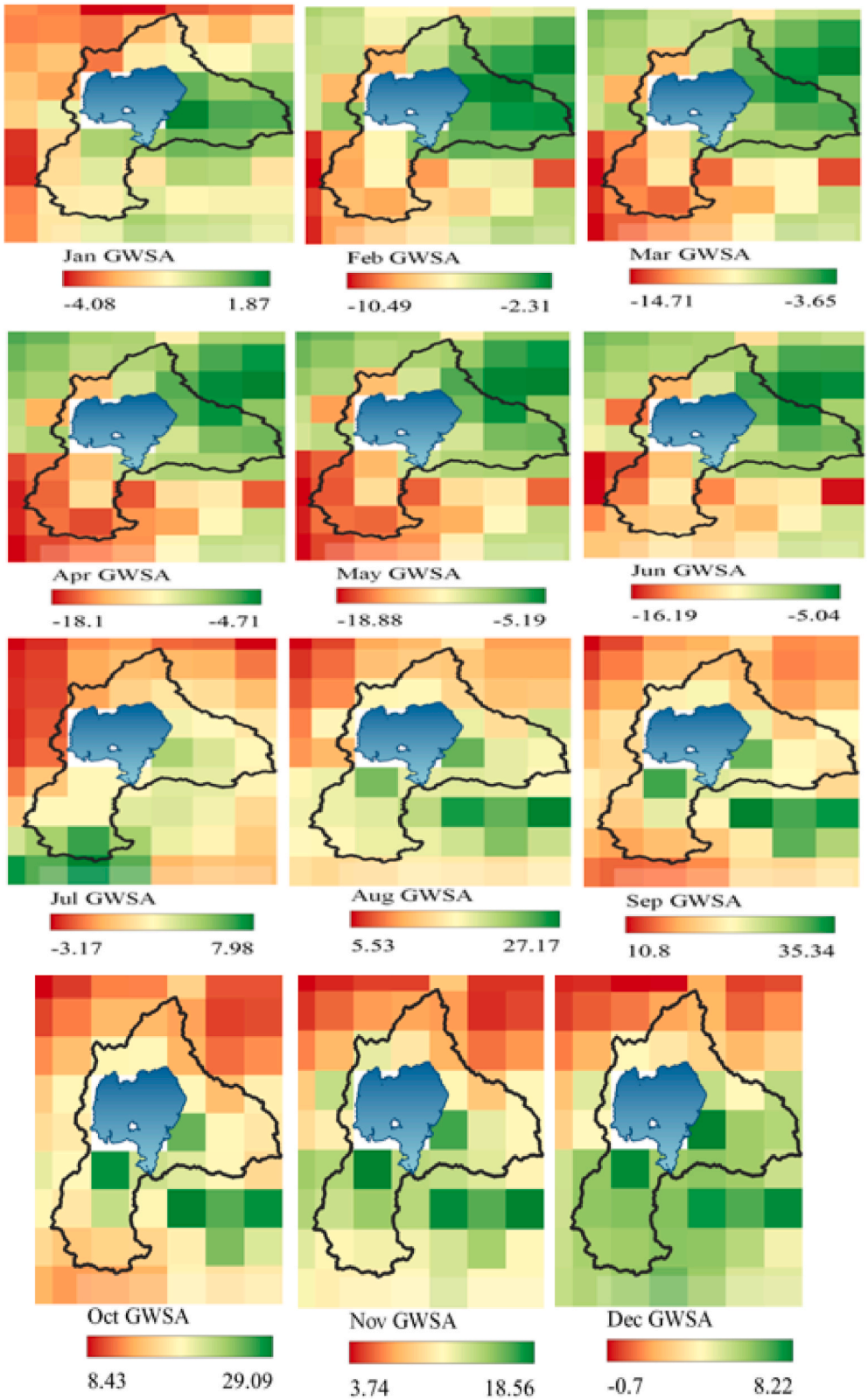

Fig. 3. The study period monthly mean GWSA spatial varations

two decades. The corresponding spatial fluctuations of 20 years of GWSA are depicted in Fig. 4.

Multi-year (two decades) monthly mean of GWSA elucidated how GWSA fluctuation behaved in the past two decades. For comparison purposes, it was depicted with a very highly correlated twenty-year monthly mean TWSA (Fig. 2 c). Fig. 2 c revealed that the study year's monthly mean GWSA dropped during the drier months (mainly from March to May) and elevated during the wet months especially from July to September ensuing the rainfall pattern. The two-decade monthly mean GWSA reached the highest positive value (20.846 cm) (groundwater gain) in September and the highest negative value (−11.998 cm) or loss in May. The great fluctuation of multi-year monthly mean GWSA was observed from June to July (12.39 cm/month) and from July to August (14.12 cm/month). The corresponding spatial variation is portrayed in Fig. 3.

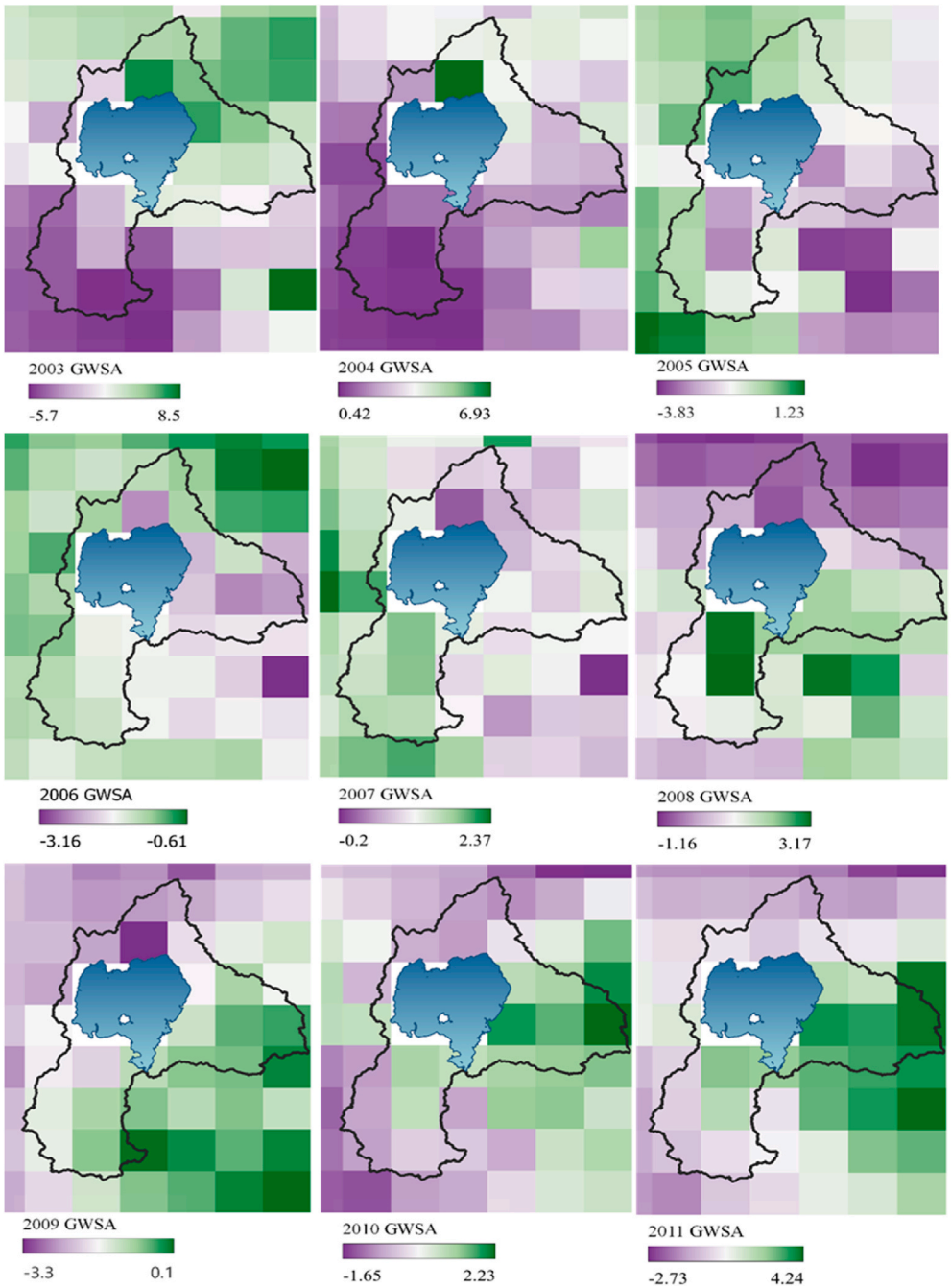

Fig. 4. The net annual GWSA spatial variations

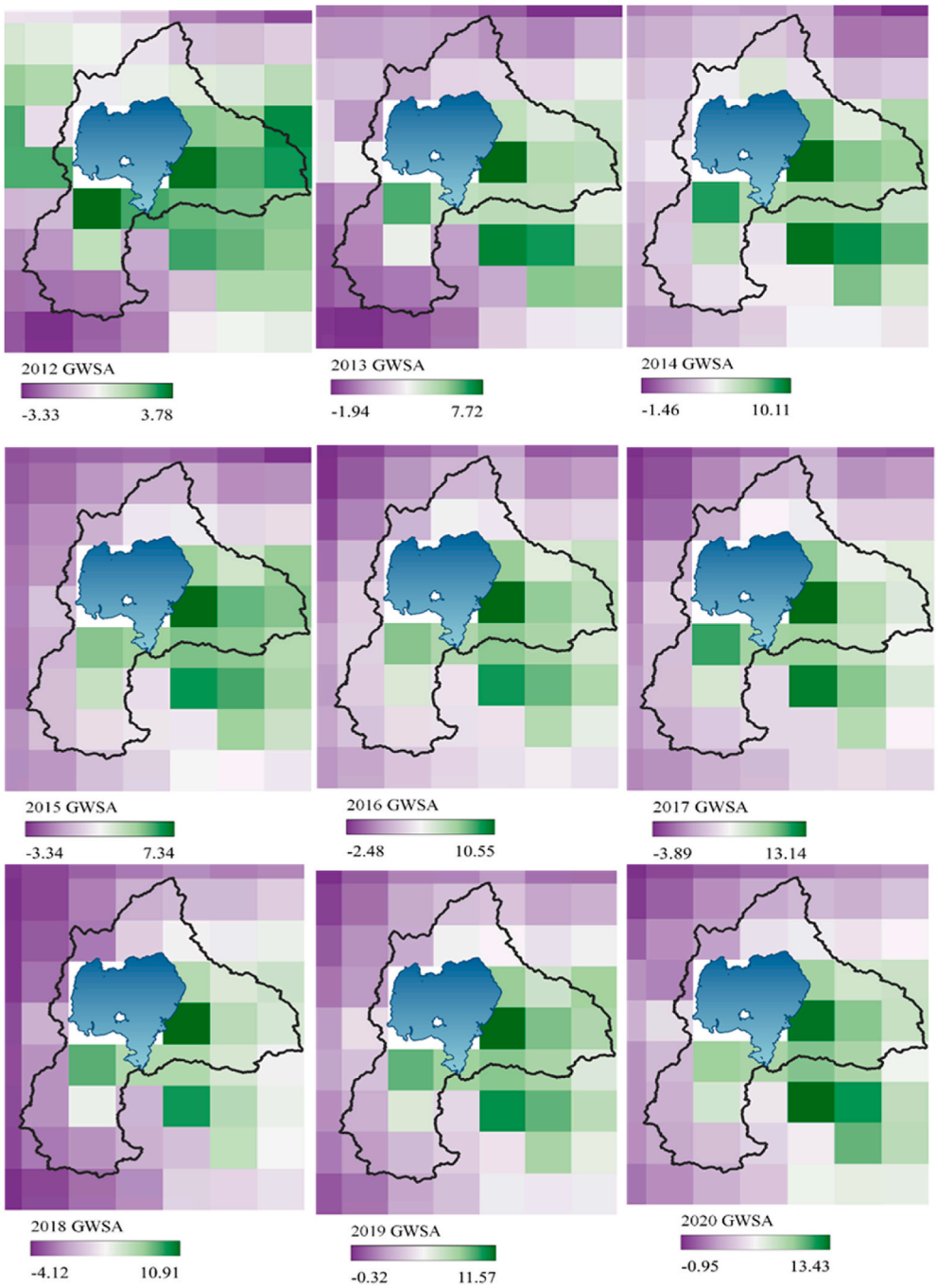

Fig. 4. (*continued*).

3.2. Spatial variations

The multi-year (2003–2022) monthly mean GWSA spatial fluctuations are presented in Fig. 3. The great spatial variation was depicted from June to July and from July to August in the near northern, southern, and eastern directions of Lake Tana. The highest deficit (−12.00 cm) of groundwater was observed in May in the southern portion of the study area. Then again, the highest groundwater gain (20.85 cm) was seen in September around the southern and eastern directions of Lake Tana.

Generally, the past two decades monthly mean GWSA displayed that the most sensitive parts of the region to noticeable fluctuations were around Lake Tana in the eastern, southern, and northern directions. This was attributed to the fact that these portions of the study area have the highest groundwater potential zones [21,23,93]. On the other hand, most of the far northern and other parts of the

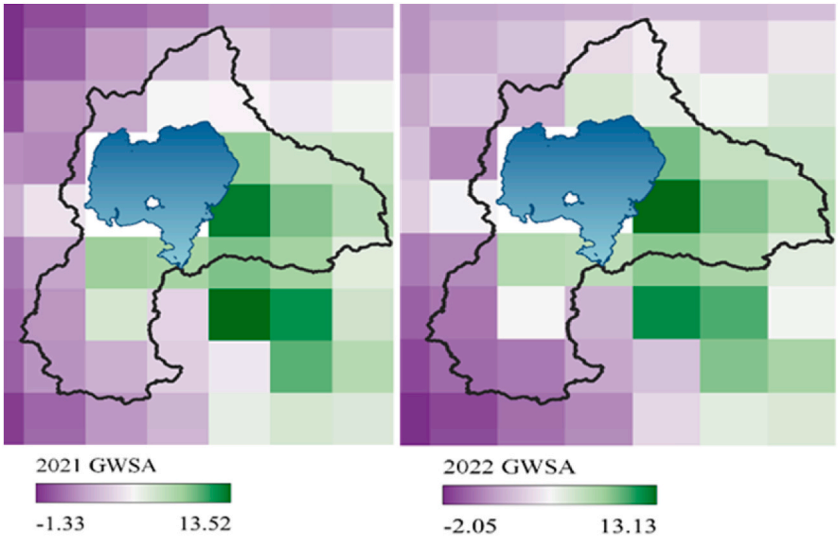

Fig. 4. (*continued*).

sub-basin revealed minor GWSA variations that pointed out the poor recharge capacity and lower groundwater potential zones [21,94].

The annual GWSA (Fig. 4) also revealed that substantial spatial variations are taking place in the vicinity of Lake Tana mainly the near southern and eastern parts. For example, net annual GWSA dropped at a rate of −3.05 cm/year from 2004 to 2005, and this was observed near Lake Tana in south and east directions. In the same fashion, when the annual GWSA rose from 2006 to 2007 (2.926 cm/year) and from 2018 to 2019 (3.545 cm/year), conspicuous increasing changes were seen in these parts of the study area. The highest gain (5.56 cm) and greatest loss (−1.69 cm) of the net annual GWSA were also recorded in the year 2020 and 2006, respectively, in these places. Further details can be inferred from Fig. 4.

3.3. Validation of GWSA

The simulated GWSA may have limitations associated with the data used. The data applied here was the CSR (Mascon solution) GRACE/GRACE-FO assimilated with GLDAS CLSM land surface model, GLDAS-2.2. The potential errors accompanied by GRACE/GRACE-FO are correlation errors, leakage errors, and errors related to the scale factors [49,95,96]. However, the CSR Mascon solution has fewer errors, which potentially come from the above-mentioned sources of errors [49,95,96]. The limitation of the GLDAS CLSM land surface model is that it can not fully estimate surface water storage (only uses runoff and canopy water as a proxy of SWS) [53,54], thereby errors may occur.

Therefore, GWSA verification with independent sort of data was carried out as follows. Groundwater fluctuations in the study region are influenced by hydrological and meteorological factors. It feeds rivers of the watershed and in turn, rivers nurture Lake Tana [25,28–30]. A past study [92] also confirmed that the TWSA of the Upper Blue Nile is strongly governed by meteorological factors mainly precipitation. Therefore, GWSA can be compared with Lake Tana level anomaly (LTLA) and precipitation anomaly (PrAn) besides the in-situ well-monitoring data to verify the simulated GWSA.

Monthly GWSA exhibited the same cyclic pattern and increasing trend as the LTLA and PrAn except for time lags. Monthly GWSA reached its highest amplitude in September, but PrAn and LTLA peaked in July and October/September, respectively (Fig. 5 a). After time lags adjustment, GWSA showed highly correlated ($R = 0.84$, $NSE = 0.29$) with LTLA, and with PrAn ($R = 0.88$, $NSE = 0.73$). The net annual GWSA also exhibited a good association with the net annual PrAn and LTLA except for some discrepancies as portrayed in Fig. 5 b. These two monthly and annual independent data anomalies experienced a significant increasing trend ($p < 0.05$) in the study period. Fig. 5 c also portrayed how the 20-year monthly mean GWSA varied with the corresponding PrAn and LTLA. Multi-year monthly mean of GWSA fluctuated consistently with PrAn and LTLA except for the speculated time lags. As conspicuously shown in Fig. 5 c, the correlation of Multi-year monthly mean GWSA with LTLA is high ($R = 0.85$), whereas with PrAn is low ($R = 0.33$).

Besides, GWSA validation was computed with observed groundwater storage anomaly ($GWSA_{obs}$) derived from eight in-situ measured groundwater levels at the end of the study period. The correlation analysis was carried out between each GWSA that was computed at each monitoring point and the respective $GWSA_{obs}$. The analysis results revealed a high to very high correlation (R ranged from 0.78 to 0.96), demonstrating nearly the same fluctuation pattern. The WW-GWSA, which was simulated at the point of WW monitoring point, was highly correlated ($R = 0.78$) with the observed WW-derived GWSA (WW-$GWSA_{obs}$) (Fig. 6 a). A very high correlation ($R = 0.96$) was also recorded between DrW-GWSA and DrW-$GWSA_{obs}$ (Fig. 6 a).

On the other hand, the highest fit ($NSE = 0.85$) was observed between WaW-GWSA and WaW-$GWSA_{obs}$ (Fig. 6 b). Above all, the best fit ($R = 0.95$ and $NSE = 0.85$) was also observed between the WaW-GWSA and WaW-$GWSA_{obs}$. The greater values of NSE and R at

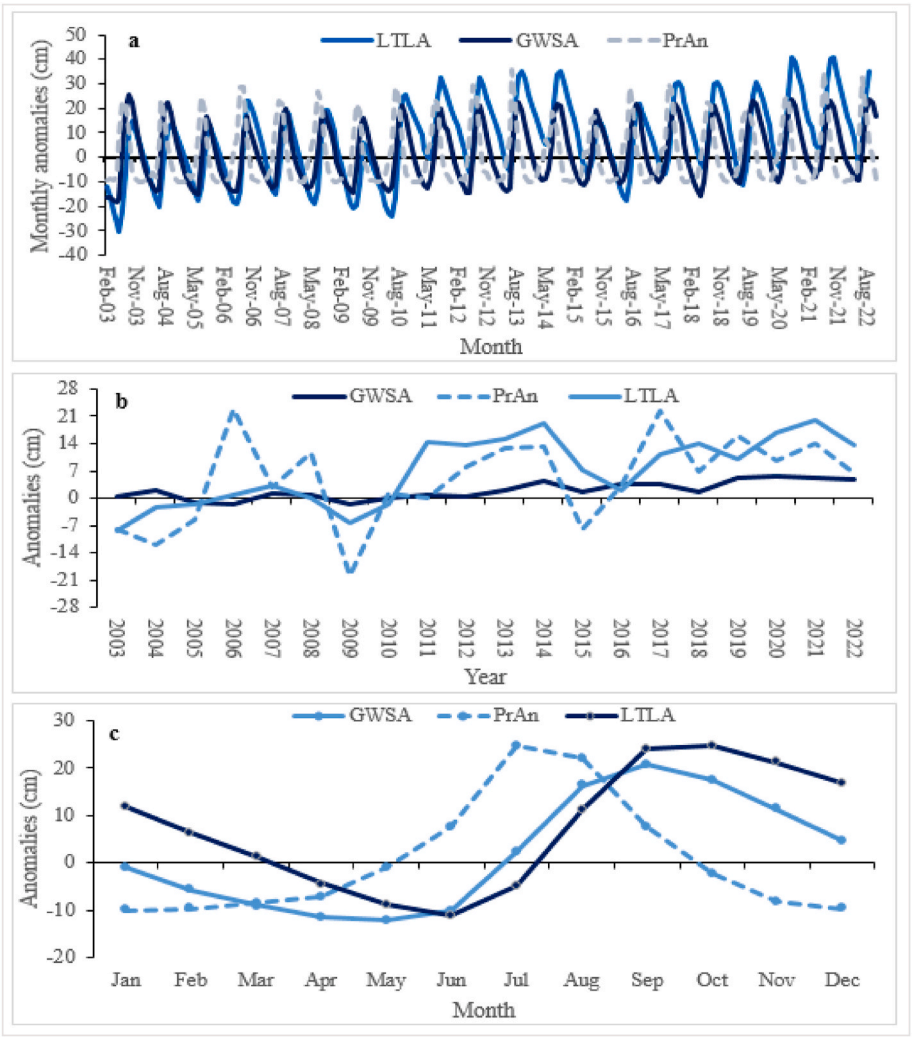

Fig. 5. Monthly (**a**), net annual (**b**), and monthly mean (**c**) of GWSA, PrAn, and LTLA.

the same time indicated that the simulated GWSA and $GWSA_{obs}$ exhibited similar temporal fluctuation pattern and amplitude as well. The estimated GWSA and $GWSA_{obs}$ at the WaW and AMW monitoring wells were the best examples compared to others (Fig. 6 b). On the other hand, the greater values of R, but relatively less values of NSE (for instance, Fig. 6 c) pointed out the greater magnitude difference between the calculated GWSA and $GWSA_{obs}$. Fig. 6 d also showed very high correlation (R = 0.9) between the simulated GWSA and the $GWSA_{obs}$, which was calculated based on the water table fluctuation method. Generally, the validation results revealed that the simulated GWSA is the plausible result in the present study area.

3.4. Discussions

In the present study, efforts have been made to evaluate the spatial and temporal dynamics of groundwater, GWSA in the Tana sub-basin. This research is the first of its kind in the Tana-sub basin applying the latest GLDAS version (GLDAS-2.2). The current study provides good insights into the temporal cyclic patterns, spatial variations, and the factors affecting GWSA for the past two decades.

The monthly GWSA (Fig. 2 a), throughout the study years, showed the annual fluctuation following the rainfall pattern. This indicated that rainfall is the main source of recharge for the unconfined aquifers-dominated region, the Tana sub-basin. This is in line with related research done in this region [21]. As described above in the validation of the GWSA section, GWSA fluctuation exhibited a strong connection with the rainfall and the Lake Tana water anomalies that are governed by climatic events [92]. The absence of recharge and the increased use of groundwater mainly for domestic and irrigation activities in the dry months might be the main reasons for groundwater loss in the region [97,98].

In the first decade of the study period, 0.49 BCM groundwater loss occurred in the three years including 2005, 2006, and 2009 (Fig. 2 b). The negative values of the net annual GWSA (groundwater loss) in the year 2006 were observed while the corresponding

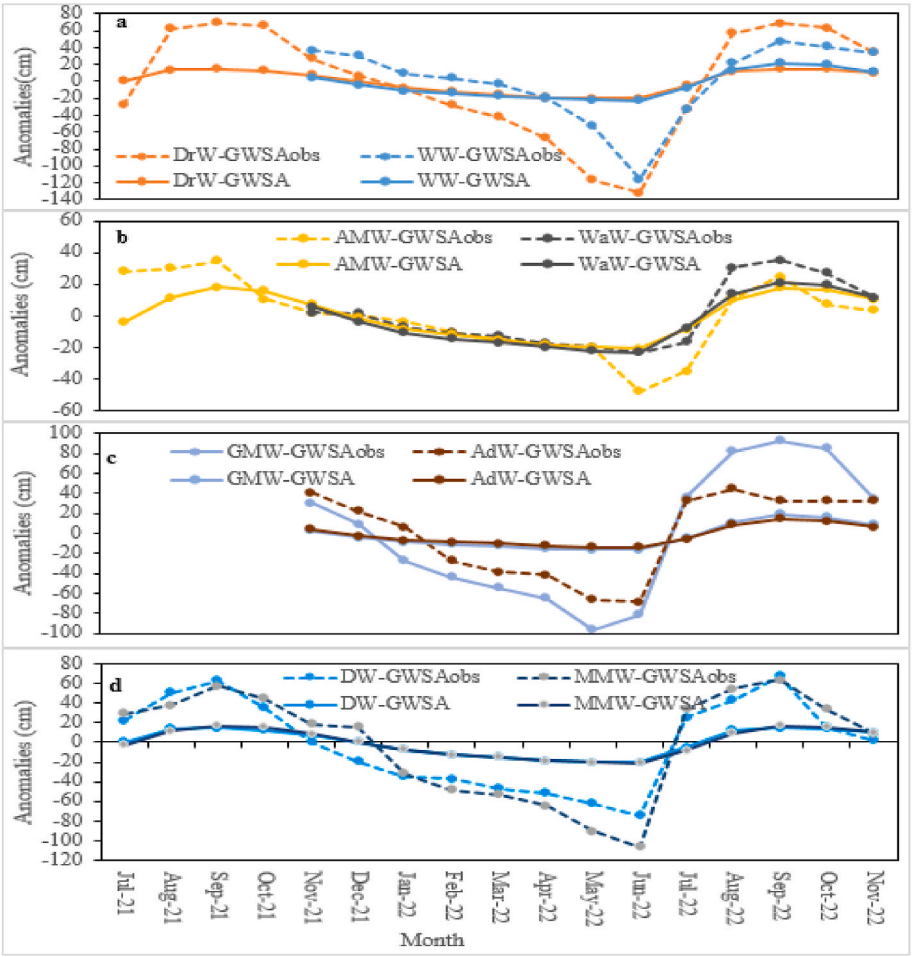

Fig. 6. Comparison between simulated GWSA and observed GWSA: (**a**) subplot portrays the relation between DrW-GWSA and DrW-GWSA$_{obs}$ (R = 0.96 and NSE = 0.36), and between WW-GWSA and WW-GWSA$_{obs}$ (R = 0.78 and NSE = 0.41); (**b**) the relation between AMW- GWSA and AMW-GWSA$_{obs}$ (R = 0.8, NSE = 0.6), and between WaW-GWSA, and WaW-GWSA$_{obs}$ (R = 0.95, NSE = 0.85); (**c**) the relation between GMW-GWSA and GMW-GWSA$_{obs}$ (R = 0.95, NSE = 0.33), and between AdW-GWSA and AdW-GWSA$_{obs}$ (R = 0.86, NSE = 0.35); (**d**) the relation between DW-GWSA and DW-GWSA$_{obs}$ (R = 0.9, NSE = 0.45), and between MMW-GWSA and MMW-GWSA$_{obs}$ (R = 0.9, NSE = 0.4).

PrAn and LTLA showed positive values (Fig. 5 b). This might be due to the effects of consecutive negative values of the net PrAn and LTLA from 2003 to 2005. Groundwater loss in the years 2005 and 2009, however, was consistent with the net annual PrAn and LTLA.

The net annual PrAn showed a greater negative value in the year 2009 for which both the corresponding GWSA and LTLA responded immediately. Previous studies also testified that since precipitation is the main source of groundwater recharge, the loss of groundwater in the abovementioned years is attributed to climate events (droughts) [91,92]. It was also evidenced by the earlier work [21] that combined groundwater and soil moisture storage loss occurrence from 2003 to 2013 in the Tana sub-basin. However, after 2010, the net annual GWSA increased positively, thereby a greater amount of gain than the loss of groundwater following the net annual LTLA and PrAn (Fig. 5b). This enabled the net annual GWSA to exhibit a significantly increased trend in the entire study years. The significant increasing trend of TWSA in the present study region (from 2002 to 2020) [60] and the nearby study area (from 2002 to 2017) [91] supported the present long-term net annual GWSA trend.

The spatial multi-year monthly mean GWSA envisaged that all parts of the study area have negative values from February to June (Fig. 3). Quite the opposite, the entire study area portions have positive monthly mean GWSA from August to November (Fig. 3). This displayed the presence of groundwater recharge from precipitation during the wet season [21,99]. The multi-year monthly mean GWSA variability was higher mainly in the southern and eastern periphery of Lake Tana. This was because these parts of the study area were replenished by the high amount of rainfall [100]. The net annual GWSA maps also presented that considerable fluctuations were confined to these hotspot parts of the sub-basin. Parts of the study area around Lake Tana have flat terrain, soil types promoting recharge, relatively high rainfall, and high groundwater potential [21,23,39]. These deriving factors may be the reason that noticeable groundwater fluctuations were observed in those areas.

Verification of the simulated monthly, long-term mean monthly, and net annual GWSA were carried out and the results showed good consistencies with the corresponding precipitation and Tana Lake level anomalies. Further, the point-wise comparisons took

place using the water table fluctuation method from eight observation wells' data. The comparison exhibited similar fluctuation patterns or high correlations. However, the amplitudes of the GWSA derived from observation wells were higher than those derived from GLDAS-2.2. A similar finding was witnessed in the present case [102]. It might be due to uncertainties associated with specific yield (Sy) estimation and in-situ water table measurement imperfections [98,103]. In general, it can be comprehended that the results obtained in the study using GLDAS-2.2 are plausible; and are governed by precipitation, climatic events (droughts), anthropogenic activities, topography, and other groundwater recharge influencing factors [21,97,98,100,101].

Promoting afforestation, water harvesting techniques (for example, terracing hillsides), and recharge-enhancing irrigation methods like furrows are recommended to circumvent groundwater loss and stream reduction during droughts. The present study provides reliable decisive information to the concerned bodies for sustainable surface-groundwater management and utilization. The present study establishes groundwork for further investigations utilizing the GLDAS-2.2 land surface model to examine groundwater storage conditions for further and future examinations including the effect of climate change and land use/cover changes.

4. Conclusion and recommendation

This study assessed the long-term groundwater storage anomaly (GWSA) in the Tana sub-basin for the last 20 years period employing GLDAS-2.2 derived groundwater storage data. The spatial and temporal variability of the GWSA were assessed and the main deriving factors are precipitation and drought. The Lake Tana level fluctuation, rainfall anomaly, and in-situ groundwater level-derived anomaly were used to validate the GWSA, and the results revealed a strong correlation. The main findings were the following.

- Groundwater storage data obtained from the latest version of the GLDAS (GLDAS-2.2) land surface model is reliable for GWS variability assessments.
- The conspicuous GWSA spatial fluctuations were observed around Lake Tana, especially in the south and east directions.
- The monthly and net annual GWSA exhibited statistically significant ($p < 0.05$) increasing trend with a rate of 0.005 cm/month and 0.333 cm/year, respectively.
- The Tana sub-basin was nurtured with a net 4.87 BCM groundwater gain in the last two decades (from 2003 to 2022) study period.

Although the overall GWSA showed a significant increasing trend, this study endorses the concerned bodies to adopt recharge enhancement techniques to diminish groundwater loss and stream reduction during climatic extremes.

Data availability statement

The data for this study will be available based on individual requests to the corresponding author.

CRediT authorship contribution statement

Kibru Gedam Berhanu: Writing – original draft, Validation, Software, Methodology, Investigation, Formal analysis, Data curation, Conceptualization. **Tarun Kumar Lohani:** Writing – review & editing, Supervision, Project administration. **Samuel Dagalo Hatiye:** Writing – review & editing, Validation, Supervision, Methodology, Data curation.

Declaration of competing interest

The authors declare that they have no known competing financial interests or personal relationships that could have appeared to influence the work reported in this paper.

References

[1] L. Dhal, S. Swain, Chapter 14 - understanding and modelling the process of seawater intrusion: a review, in: P.K. Gupta, B. Yadav, S.K. Himanshu (Eds.), Adv. Remediat. Tech. Polluted Soils Groundw, Elsevier, 2022, pp. 269–290, https://doi.org/10.1016/B978-0-12-823830-1.00009-2.
[2] S. Sahoo, S. Swain, A. Goswami, R. Sharma, B. Pateriya, Assessment of trends and multi-decadal changes in groundwater level in parts of the Malwa region, Punjab, India, Groundw Sustain Dev 14 (2021) 100644, https://doi.org/10.1016/j.gsd.2021.100644.
[3] W. Yin, L. Hu, Statistical Downscaling of GRACE-Derived Groundwater Storage Using ET Data in the North China Plain, 2018, https://doi.org/10.1029/2017JD027468, 5973–87.
[4] S. Swain, A.K. Taloor, L. Dhal, S. Sahoo, N. Al-Ansari, Impact of climate change on groundwater hydrology: a comprehensive review and current status of the Indian hydrogeology, Appl. Water Sci. 12 (2022), https://doi.org/10.1007/s13201-022-01652-0.
[5] M.A. Asadi Zarch, B. Sivakumar, A. Sharma, Droughts in a warming climate: a global assessment of Standardized precipitation index (SPI) and Reconnaissance drought index (RDI), J. Hydrol. 526 (2015) 183–195, https://doi.org/10.1016/j.jhydrol.2014.09.071.
[6] A.K. Mishra, V.P. Singh, A review of drought concepts, J. Hydrol. 391 (2010) 202–216, https://doi.org/10.1016/j.jhydrol.2010.07.012.
[7] J.T. Grönwall, M. Mulenga, G. McGranahan, Groundwater, Self-Supply and Poor Urban Dwellers: A Review with Case Studies of Bangalore and Lusaka, IIED, 2010.
[8] S. Foster, Global Policy Overview of Groundwater in Urban Development — A Tale of 10 Cities !, 2020.
[9] S. Swain, S.K. Mishra, A. Pandey, P. Kalura, Inclusion of groundwater and socio-economic factors for assessing comprehensive drought vulnerability over Narmada River Basin, India: a geospatial approach, Appl. Water Sci. 12 (2022) 1–16, https://doi.org/10.1007/s13201-021-01529-8.
[10] S. Swain, S. Sahoo, A.K. Taloor, Groundwater quality assessment using geospatial and statistical approaches over Faridabad and Gurgaon districts of National Capital Region, India, Appl. Water Sci. 12 (2022) 1–14, https://doi.org/10.1007/s13201-022-01604-8.

[11] P. Doll, H.M. Schmied, C. Schuh, F.T. Portmann, A. Eicker, Global-scale assessment of groundwater depletion and related groundwater abstractions: combining hydrological modeling with information from well observations and GRACE satellites, Water Resour. Res. (2014), https://doi.org/10.1002/2013WR014979. Reply, 5375–7.
[12] Y. Wada, L.P.H. Van Beek, C.M. Van Kempen, J.W.T.M. Reckman, S. Vasak, M.F.P. Bierkens, Global depletion of groundwater resources, Geophys. Res. Lett. 37 (2010).
[13] T. Sarkar, A. Karunakalage, S. Kannaujiya, C. Chaganti, Quantification of groundwater storage variation in Himalayan & Peninsular River basins correlating with land deformation effects observed at different Indian cities, Contrib. Geophys. Geodes. 52 (2022) 1–56, https://doi.org/10.31577/CONGEO.2022.52.1.1.
[14] F.K. Khadim, Z. Dokou, R. Lazin, S. Moges, A.C. Bagtzoglou, E. Anagnostou, Groundwater modeling in data scarce aquifers: the case of Gilgel-Abay, Upper Blue Nile, Ethiopia, J. Hydrol. 590 (2020) 125214.
[15] MoWR GM. Ethiopia: strategic framework for managed groundwater development. Addis Ababa. 2011;52.
[16] MoWR, National water development report for Ethiopia (Final), Addis Ababa (2004).
[17] T. Alemayehu, Groundwater Occurrence in Ethiopia, Addis Ababa Univ Addis Ababa, Ethiop, 2006.
[18] B. Berhanu, Y. Seleshi, A.M. Melesse, Surface Water and Groundwater Resources of Ethiopia: Potentials and Challenges of Water Resources Development, Springer, Nile River Basin, 2014, pp. 97–117.
[19] G.G. Haile, A.K. Kassa, Irrigation in Ethiopia, a review, J. Environ. Earth Sci. 3 (2015) 264–269.
[20] Pavelic P, Giordano M, Keraita B, Ramesh V, Rao T. Groundwater Availability and Use in Sub-saharan Africa: A Review of 15 Countries. Colombo, Sri Lanka : International Management Institute (IWMI). 274 p. doi: 10.5337/2012.213.2012..
.[21]A.Z. Abiy, A.M. Melesse, Evaluation of watershed scale changes in groundwater and soil moisture storage with the application of GRACE satellite imagery data Catena Evaluation of watershed scale changes in groundwater and soil moisture storage with the application of GRACE satellite, Catena (2017), https://doi.org/10.1016/j.catena.2017.01.036.
[22] T. Ayenew, M. Demlie, S. Wohnlich, Hydrogeological framework and occurrence of groundwater in the Ethiopian aquifers, J. Afr. Earth Sci. 52 (2008) 97–113.
[23] A.T. Kindie, T. Enku, M.A. Moges, Spatial Analysis of Groundwater Potential Using GIS Based Multi Criteria Decision Analysis Method in Lake Tana Basin, Ethiopia : 6th EAI International Spatial Analysis of Groundwater Potential Using GIS Based Multi Criteria Decision Analysis Method in La, Springer International Publishing, 2019, https://doi.org/10.1007/978-3-030-15357-1.
[24] A. Abera, N.E.C. Verhoest, S. Tilahun, H. Inyang, J. Nyssen, Assessment of irrigation expansion and implications for water resources by using RS and GIS techniques in the Lake Tana Basin of Ethiopia, Environ. Monit. Assess. 193 (2021) 1–17, https://doi.org/10.1007/s10661-020-08778-1.
[25] A.Z. Abiy, S.S. Demissie, C. Macalister, S.B. Dessu, A.M. Melesse, Groundwater Recharge and Contribution to the Tana Sub-basin , Upper Blue Nile Á Recharge Á SWAT Á T-Plot Á, 2016, https://doi.org/10.1007/978-3-319-18787-7, 463–81.
[26] F. Nigate, M. Van Camp, S. Kebede, K. Walraevens, Hydrologic interconnection between the volcanic aquifer and springs, Lake Tana basin on the upper Blue nile, J. Afr. Earth Sci. 121 (2016) 154–167, https://doi.org/10.1016/j.jafrearsci.2016.05.015.
[27] H.B. Wakode, K. Baier, R. Jha, R. Azzam, Impact of urbanization on groundwater recharge and urban water balance for the city of Hyderabad, India, Int Soil Water Conserv Res 6 (2018) 51–62, https://doi.org/10.1016/j.iswcr.2017.10.003.
[28] S. Mamo, T. Ayenew, B. Berehanu, K. Seifu, Hydrology of the Lake Tana basin , Ethiopia : implication to groundwater- hydrology of the Lake Tana basin , Ethiopia, J. Environ. Earth Sci. 6 (2016) 2224–3216.
[29] T.B. Tigabu, P.D. Wagner, G. Hörmann, N. Fohrer, Modeling the spatio-temporal flow dynamics of groundwater-surface water interactions of the Lake Tana basin, upper Blue nile, Ethiopia, Nord. Hydrol 51 (2020) 1537–1559, https://doi.org/10.2166/nh.2020.046.
[30] D. Walker, G. Parkin, J. Gowing, A.T. Haile, Development of a hydrogeological conceptual model for shallow aquifers in the data scarce upper Blue Nile basin, Hydrology 6 (2019), https://doi.org/10.3390/hydrology6020043.
[31] H. Chen, W. Zhang, N. Nie, Y. Guo, Long-term groundwater storage variations estimated in the Songhua River Basin by using GRACE products , land surface models , and in-situ observations, Sci. Total Environ. 649 (2019) 372–387, https://doi.org/10.1016/j.scitotenv.2018.08.352.
[32] M. Shukla, V. Maurya, R. Dwivedi, Groundwater monitoring using grace mission, Int. Arch. Photogramm. Remote Sens. Spat. Inf. Sci. - ISPRS Arch. 43 (2021) 425–430, https://doi.org/10.5194/isprs-archives-XLIII-B3-2021-425-2021.
[33] F. Frappart, G. Ramillien, Monitoring Groundwater Storage Changes Using the Gravity Recovery and Climate Experiment (GRACE) Satellite Mission: A Review, vol. 3, 2018, https://doi.org/10.3390/rs10060829.
[34] M.D. Melati, A.S. Fleischmann, F.M. Fan, R.C.D. Paiva, G.B. Athayde, Estimates of groundwater depletion under extreme drought in the Brazilian semi-arid region using GRACE satellite data: application for a small-scale aquifer, Hydrogeol. J. 27 (2019) 2789–2802, https://doi.org/10.1007/s10040-019-02065-1.
[35] A.Y. Sun, Predicting Groundwater Level Changes Using GRACE Data, vol. 49, 2013, pp. 5900–5912, https://doi.org/10.1002/wrcr.20421.
[36] Z. Duan, H. Gao, C. Ke, Estimation of Lake outflow from the poorly gauged Lake Tana (Ethiopia) using satellite remote sensing data, Rem. Sens. 10 (2018) 1060.
[37] M.T. Taye, P. Willems, Temporal variability of hydroclimatic extremes in the Blue Nile basin, Water Resour. Res. 48 (2012).
[38] W.B. Abebe, G/Michael T, E.S. Leggesse, B.S. Beyene, F. Nigate, Climate of Lake Tana basin, in: K. Stave al (Ed.), Soc. Ecol. Syst. Dyn. AESS Interdiscip, Environ. Stud. Sci. Ser., 2017, pp. 51–58, https://doi.org/10.1007/978-3-319-45755-0_5.
[39] K.G. Berhanu, S.D. Hatiye, T.K. Lohani, Coupling support vector machine and the irrigation water quality index to assess groundwater quality suitability for irrigation practices in the Tana sub-basin, Ethiopia, Water Pract. Technol. 18 (2023) 884–900, https://doi.org/10.2166/wpt.2023.055.
[40] S.G. Setegn, R. Srinivasan, A.M. Melesse, B. Dargahi, SWAT model application and prediction uncertainty analysis in the Lake Tana Basin, Ethiopia, Hydrol Process An Int J 24 (2010) 357–367.
[41] GSE, Geology, Geochemistry and Gravity Survey of Gondar and West Gondar Map Sheets (ND 37/13 & ND 36/16), 2011.
[42] GSE, Integrated Hydrogeological and Hydrochemical Mapping of Yifag Map Sheet (ND 37-14) (Unpublished), 2013. Addis Ababa, Ethiopia.
[43] SMEC, Hydrological Study of the Tana-Beles Sub-basins, Surf Water Investig MOWR Addis Ababa, Ethiop, 2008.
[44] B.D. Tapley, S. Bettadpur, M. Watkins, C. Reigber, The gravity recovery and climate experiment: mission overview and early results, Geophys. Res. Lett. 31 (2004) L09607, https://doi.org/10.1029/2004GL019920.
[45] F.W. Landerer, F.M. Flechtner, H. Save, F.H. Webb, T. Bandikova, W.I. Bertiger, et al., Extending the global mass change data record: GRACE Follow-On instrument and science data performance, Geophys. Res. Lett. 47 (2020) e2020GL088306.
[46] F.W. Landerer, S.C. Swenson, Accuracy of scaled GRACE terrestrial water storage estimates, Water Resour. Res. 48 (2012) W04531, https://doi.org/10.1029/2011WR011453.
[47] J. Wahr, M. Molenaar, F. Bryan, Time variability of the Earth's gravity field: hydrological and oceanic effects and their possible detection using GRACE, J. Geophys. Res. B 103 (12) (1998) 30205–30229.
[48] B.R. Scanlon, Z. Zhang, H. Save, D.N. Wiese, F.W. Landerer, D. Long, et al., Global evaluation of new GRACE mascon products for hydrologic applications, Water Resour. Res. 52 (2016) 9412–9429.
[49] H. Save, S. Bettadpur, B.D. Tapley, High-resolution CSR GRACE RL05 mascons, J. Geophys. Res. Solid Earth 121 (2016) 7547–7569.
[50] B. Li, M. Rodell, S. Kumar, H.K. Beaudoing, A. Getirana, F. Zaitchik B, et al., Global GRACE data assimilation for groundwater and drought monitoring: advances and challenges, Water Resour. Res. (2019), https://doi.org/10.1029/2018WR024618.
[51] Z.M. Nigatu, D. Fan, W. You, Integrating GRACE Products and Land Surface Models to Estimate Changes in Key Components of Terrestrial Water Storage in the Nile River Basin, 2020.
[52] M. Rodell, P.R. Houser, U.E.A. Jambor, J. Gottschalck, K. Mitchell, C.-J. Meng, et al., The global land data assimilation system, Bull. Am. Meteorol. Soc. 85 (2004) 381–394.
[53] K. Sun, L. Hu, X. Liu, W. Yin, Reconstructing terrestrial water storage anomalies using satellite data to evaluate water resource shortages from 1980 to 2016 in the Inland Yongding River Basin, China, Geofluids (2021) 2021, https://doi.org/10.1155/2021/7275242.

[54] J. Xiong, J. Yin, S. Guo, L. Slater, Continuity of terrestrial water storage variability and trends across mainland China monitored by the GRACE and GRACE-Follow on satellites, J. Hydrol. 599 (2021) 126308, https://doi.org/10.1016/j.jhydrol.2021.126308.
[55] X. Liang, D.P. Lettenmaier, E.F. Wood, S.J. Burges, A simple hydrologically based model of land surface water and energy fluxes for general circulation models, J. Geophys. Res. Atmos. 99 (1994) 14415–14428.
[56] R.D. Koster, M.J. Suarez, Energy and Water Balance Calculations in the Mosaic LSM. National Aeronautics and Space Administration, Goddard Space Flight Center, 1996.
[57] Y. Dai, X. Zeng, R.E. Dickinson, I. Baker, G.B. Bonan, M.G. Bosilovich, et al., The common land model, Bull. Am. Meteorol. Soc. 84 (2003) 1013–1023, https://doi.org/10.1175/BAMS-84-8-1013.
[58] F. Chen, K. Mitchell, J. Schaake, Y. Xue, H.L. Pan, V. Koren, et al., Modeling of land surface evaporation by four schemes and comparison with FIFE observations, J. Geophys. Res. 101 (1996) 7251–7268, https://doi.org/10.1029/95JD02165.
[59] V. Koren, J. Schaake, K. Mitchell, Q.-Y. Duan, F. Chen, J.M. Baker, A parameterization of snowpack and frozen ground intended for NCEP weather and climate models, J. Geophys. Res. Atmos. 104 (1999) 19569–19585.
[60] E. Hasan, A. Tarhule, P.E. Kirstetter, Twentieth and twenty-first century water storage changes in the nile river basin from grace/grace-fo and modeling, Rem. Sens. 13 (2021) 1–30, https://doi.org/10.3390/rs13050953.
[61] S. Wang, J. Li, H.J. Russell, Methods for estimating surface water storage changes and their evaluations, J. Hydrometeorol. 24 (2023) 445–461, https://doi.org/10.1175/jhm-d-22-0098.1.
[62] H.L. Rui, H. Beaudoing, README document for NASA GLDAS version 2 data products, Goddard Earth Sci. Data Inf. Serv. Cent. (GES DISC) 16 (2020) 1–32.
[63] S. Calmant, F. Seyler, J.F. Cretaux, Monitoring continental surface waters by satellite altimetry, Surv. Geophys. 29 (2008) 247–269.
[64] J.-F. Crétaux, W. Jelinski, S. Calmant, A. Kouraev, V. Vuglinski, M. Bergé-Nguyen, et al., SOLS: a lake database to monitor in the Near Real Time water level and storage variations from remote sensing data, Adv. Space Res. 47 (2011) 1497–1507.
[65] S. Ni, J. Chen, C.R. Wilson, X. Hu, Long-term water storage changes of Lake Volta from GRACE and satellite altimetry and connections with regional climate, Rem. Sens. 9 (2017) 1–15, https://doi.org/10.3390/rs9080842.
[66] G. Zhang, H. Xie, S. Kang, D. Yi, S.F. Ackley, Monitoring lake level changes on the Tibetan Plateau using ICESat altimetry data (2003–2009), Remote Sens. Environ. 115 (2011) 1733–1742.
[67] A. Belayneh, G. Sintayehu, K. Gedam, T. Muluken, Evaluation of satellite precipitation products using HEC-HMS model, Model Earth Syst. Environ. 6 (2020), https://doi.org/10.1007/s40808-020-00792-z.
[68] M.T. Taye, A.T. Haile, A.G. Fekadu, P. Nakawuka, Effect of irrigation water withdrawal on the hydrology of the Lake Tana Sub-basin, J. Hydrol. Reg. Stud. 38 (2021) 100961, https://doi.org/10.1016/j.ejrh.2021.100961.
[69] C.S. Chanu, H. Munagapati, V.M. Tiwari, A. Kumar, L. Elango, Use of GRACE time-series data for estimating groundwater storage at small scale, J. Earth Syst. Sci. 129 (2020), https://doi.org/10.1007/s12040-020-01465-2.
[70] S.N. Bhanja, X. Zhang, J. Wang, Estimating Long-Term Groundwater Storage and its Controlling Factors in Alberta, Canada, 2018, 6241–55.
[71] D.A. Morris, A.I. Johnson, Summary of Hydrologic and Physical Properties of Rock and Soil 40 Materials, as Analyzed by the Hydrologic Laboratory of the US Geological Survey, 1948-60 (No.41 1839-D), US Govt. Print. Off, 1967.
[72] D.K. Todd, L.W. Mays, Groundwater Hydrology, third ed., vol. 636, John Wiley & Sons, NJ, 2005, p. 43.
[73] M.G. Kendall, Rank Correlation Methods, Charles Griffin, London, 1975, p. 202.
[74] H.B. Mann, Nonparametric tests against trend, Econometrica 13 (3) (1945) 245–259.
[75] K.H. Hamed, A.R. Rao, A modified Mann-Kendall trend test for autocorrelated data, J. Hydrol. 204 (1998) 182–196.
[76] P.K. Sen, Estimates of the regression coefficient based on Kendall's tau, J. Am. Stat. Assoc. 63 (324) (1968) 1379–1389.
[77] R. Mirabbasi, F. Ahmadi, D. Jhajharia, Comparison of parametric and non-parametric methods for trend identi fi cation in groundwater levels in Sirjan plain aquifer, Iran Rasoul Mirabbasi, Farshad Ahmadi and Deepak Jhajharia, Nord. Hydrol (2020), https://doi.org/10.2166/nh.2020.041.
[78] S. Swain, S. Sahoo, A.K. Taloor, S.K. Mishra, A. Pandey, Exploring recent groundwater level changes using Innovative Trend Analysis (ITA) technique over three districts of Jharkhand, India, Groundw Sustain Dev 18 (2022) 100783, https://doi.org/10.1016/j.gsd.2022.100783.
[79] S. Swain, D. Dayal, A. Pandey, S.K. Mishra, Trend Analysis of Precipitation and Temperature for Bilaspur District, Chhattisgarh, India, World Environ Water Resour Congr 2019 (2019) 193–204, https://doi.org/10.1061/9780784482346.020, 2019 Groundwater, Sustain Hydro-Climate/Climate Chang Environ Eng - Sel Pap from World Environ Water Resour Congr.
[80] S. Swain, S.K. Mishra, A. Pandey, Assessing spatiotemporal variation in drought characteristics and their dependence on timescales over Vidarbha Region, India, Geocarto Int. 37 (2022) 17971–17993, https://doi.org/10.1080/10106049.2022.2136260.
[81] S. Swain, S.K. Mishra, A. Pandey, A detailed assessment of meteorological drought characteristics using simplified rainfall index over Narmada River Basin, India, Environ. Earth Sci. 80 (2021) 1–15, https://doi.org/10.1007/s12665-021-09523-8.
[82] S. Swain, S.K. Mishra, A. Pandey, P.K. Srivastava, S. Nandi, Characterization and assessment of hydrological droughts using GloFAS streamflow data for the Narmada River Basin, India, Environ. Sci. Pollut. Res. (2023), https://doi.org/10.1007/s11356-023-27036-8.
[83] S. Swain, S.K. Mishra, A. Pandey, D. Dayal, Spatiotemporal assessment of precipitation variability, seasonality, and extreme characteristics over a Himalayan catchment, Theor. Appl. Climatol. 147 (2022) 817–833, https://doi.org/10.1007/s00704-021-03861-0.
[84] G.C. Guptha, S. Swain, N. Al-Ansari, A.K. Taloor, D. Dayal, Evaluation of an urban drainage system and its resilience using remote sensing and GIS, Remote Sens Appl Soc Environ 23 (2021), https://doi.org/10.1016/j.rsase.2021.100601.
[85] S. Swain, S.K. Mishra, A. Pandey, D. Dayal, Assessment of drought trends and variabilities over the agriculture-dominated Marathwada Region, India, Environ. Monit. Assess. (2022) 194, https://doi.org/10.1007/s10661-022-10532-8.
[86] M.R.I. Baig, M.W. Naikoo, A.H. Ansari, S. Ahmad, A. Rahman, Spatio-temporal analysis of precipitation pattern and trend using standardized precipitation index and Mann–Kendall test in coastal Andhra Pradesh, Model Earth Syst. Environ. 8 (2021) 2733–2752.
[87] H. Jiqin, F.T. Gelata, S. Chaka Gemeda, Application of MK trend and test of Sen's slope estimator to measure impact of climate change on the adoption of conservation agriculture in Ethiopia, J. Water Clim. Chang. 14 (2023) 977–988, https://doi.org/10.2166/wcc.2023.508.
[88] T.M. Aschale, D.J. Peres, A. Gullotta, G. Sciuto, A. Cancelliere, Trend analysis and identification of the meteorological factors influencing reference evapotranspiration, Water (Switzerland) 15 (2023) 1–17, https://doi.org/10.3390/w15030470.
[89] D.N. Moriasi, J.G. Arnold, M.W. Van Liew, R.L. Bingner, R.D. Harmel, T.L. Veith, Model evaluation guidelines for systematic quantification of accuracy in watershed simulations, Trans. ASABE (Am. Soc. Agric. Biol. Eng.) 50 (2007) 885–900.
[90] K.G. Calkins, Applied Statistics - Lesson 5 : Correlation Coefficients, 2005. https://www.andrews.edu/~calkins/math/edrm611/edrm05.htm. (Accessed 18 May 2005).
[91] Y.S. Getahun, M.-H. Lib, Y.-Y. Chenc, T.A. Yated, Drought characterization and severity analysis using GRACE-TWS and MODIS datasets : a case study from the Awash River Basin (ARB), Ethiopia, Water Clim. Chang 14 (2023) 516–542, https://doi.org/10.2166/wcc.2023.361.
[92] W.M. Seyoum, Characterizing water storage trends and regional climate influence using GRACE observation and satellite altimetry data in the Upper Blue Nile River Basin, J. Hydrol. 566 (2018) 274–284, https://doi.org/10.1016/j.jhydrol.2018.09.025.
[93] K.G. Berhanu, S.D. Hatiye, Identification of groundwater potential zones using proxy data : case study of megech watershed , Ethiopia, J. Hydrol. Reg. Stud. 28 (2020), https://doi.org/10.1016/j.ejrh.2020.100676.
[94] B. Das, S.C. Pal, S. Malik, R. Chakrabortty, Modeling groundwater potential zones of Puruliya district, West Bengal, India using remote sensing and GIS techniques, Geol. Ecol. Landscapes 3 (2019) 223–237.
[95] M. Schumacher, J. Kusche, P. Döll, A systematic impact assessment of GRACE error correlation on data assimilation in hydrological models, J. Geodyn. 90 (2016) 537–559, https://doi.org/10.1007/s00190-016-0892-y.
[96] J. Chen, B. Tapley, M.E. Tamisiea, H. Save, C. Wilson, S. Bettadpur, et al., Error assessment of GRACE and GRACE follow-on mass change, J. Geophys. Res. Solid Earth 126 (2021) 1–18, https://doi.org/10.1029/2021JB022124.

[97] S. Mamo, B. Birhanu, T. Ayenew, G. Taye, Three-dimensional groundwater flow modeling to assess the impacts of the increase in abstraction and recharge reduction on the groundwater, groundwater availability and groundwater-surface waters interaction: a case of the rib catchment in the Lake Tana s, J. Hydrol. Reg. Stud. 35 (2021) 100831, https://doi.org/10.1016/j.ejrh.2021.100831.
[98] A.Y. Yimam, F.K. Sishu, T.T. Assefa, T.S. Steenhuis, M.R. Reyes, R. Srinivasan, et al., Modifying the water table fluctuation method for calculating recharge in sloping aquifers, J. Hydrol. Reg. Stud. 46 (2023) 101325, https://doi.org/10.1016/j.ejrh.2023.101325.
[99] N.O. Agutu, J.L. Awange, C. Ndehedehe, F. Kirimi, M. Kuhn, GRACE-derived groundwater changes over Greater Horn of Africa: temporal variability and the potential for irrigated agriculture, Sci. Total Environ. 693 (2019) 133467, https://doi.org/10.1016/j.scitotenv.2019.07.273.
[100] A. Yenehun, M. Dessie, F. Nigate, A.S. Belay, M. Azeze, M Van Camp, et al., Spatial and temporal simulation of groundwater recharge and cross-validation with point estimations in volcanic aquifers with variable topography, J. Hydrol. Reg. Stud. 42 (2022) 101142, https://doi.org/10.1016/j.ejrh.2022.101142.
[101] T. Abraha, A. Tibebu, G. Ephrem, Rapid urbanization and the growing water risk challenges in Ethiopia: the need for water sensitive thinking, Front Water 4 (2022) 1–19, https://doi.org/10.3389/frwa.2022.890229.
[102] S. Wang, H. Liu, Y. Yu, W. Zhao, Q. Yang, J. Liu, Evaluation of groundwater sustainability in the arid Hexi Corridor of Northwestern China, using GRACE, GLDAS and measured groundwater data products, Sci. Total Environ. 705 (2020) 135829, https://doi.org/10.1016/j.scitotenv.2019.135829.
[103] Y. Hajhouji, Y. Fakir, S. Gascoin, V. Simonneaux, A. Chehbouni, Dynamics of groundwater recharge near a semi-arid Mediterranean intermittent stream under wet and normal climate conditions, J. Arid Land 14 (2022) 739–752, https://doi.org/10.1007/s40333-022-0067-z.